Cell, Vol. 116, 393–404, February 6, 2004, Copyright ©2004 by Cell Press

The Structural Mechanism of Translocation and Helicase Activity in T7 RNA Polymerase

Y. Whitney Yin[1,4] and Thomas A. Steitz[1,2,3,*]
[1]Department of Molecular Biophysics and Biochemistry
[2]Department of Chemistry
Yale University
[3]Howard Hughes Medical Institute
New Haven, Connecticut 06520

Summary

RNA polymerase functions like a molecular motor that can convert chemical energy into the work of strand separation and translocation along the DNA during transcription. The structures of phage T7 RNA polymerase in an elongation phase substrate complex that includes the incoming nucleoside triphosphate and a pretranslocation product complex that includes the product pyrophosphate (PP_i) are described here. These structures and the previously determined posttranslocation elongation complex demonstrate that two enzyme conformations exist during a cycle of single nucleotide addition. One orientation of a five-helix subdomain is stabilized by the phosphates of either the incoming NTP or by the product PP_i. A second orientation of this subdomain is stable in their absence and is associated with translocation of the heteroduplex product as well as strand separation of the downstream DNA. We propose that the dissociation of the product PP_i after nucleotide addition produces the protein conformational change resulting in translocation and strand separation.

Introduction

A major deficiency in our understanding of DNA-dependent RNA polymerases, indeed all polynucleotide polymerases, is the structural and energetic mechanism by which translocation of the duplex product and separation of the duplex strands are achieved. During the initiation phase of transcription, RNAP binds to promoter DNA, opens the duplex strands, and initiates transcription at specific sites (von Hippel, 1998; von Hippel et al., 1984). As nucleotides are incorporated into the growing RNA transcript, the polymerase scrunches the DNA template while opening the downstream duplex and ultimately undergoes a conformational change that converts it from an initiation to an elongation phase (Cheetham and Steitz, 1999; Tahirov et al., 2002; Yin and Steitz, 2002) after synthesis of an approximately 8 to 12 nucleotide long transcript (Huang and Sousa, 2000; Ikeda and Richardson, 1986). This conformational change results in the release of the promoter from the polymerase. During the elongation phase of transcription, synthesis is completely processive to the end of the transcript, which is also progressively peeled off the template strand as synthesis proceeds (Dedrick et al., 1987; Lorch et al., 1987; Martin et al., 1988).

RNA synthesis occurs through cycles of repeated ribonucleotide incorporation (Figure 1A). Each single nucleotide addition cycle can be divided into at least four steps. (1) and (2) Substrate NTP binds to the polymerase in a preinsertion mode followed by occupancy of the NTP binding site, or N site. The 3′ end of RNA is in the priming site or P site (Krakow and Fronk, 1969). (3) The phosphoryl transfer reaction yields the products pyrophosphate (PP_i) and the RNA transcript that has been extended by one nucleotide into the N site. (4) The elongated primer-template translocates relative to the catalytic residues and in this process, the 3′ end of the RNA moves from the N site into the P site, vacating the N site for the next cycle of nucleotide addition.

Several models have been advanced for the mechanism of the translocation. One hypothesis, called the power stroke mechanism (Jiang and Sheetz, 1994), proposes that the energy for translocation is derived ultimately from the NTP to be incorporated and is converted into mechanical energy through conformational changes in the polymerase. Similar mechanisms have been proposed for the movement of myosin along actin filaments as well as kinesin moving along microtubules (Reedy, 2000; Tyska and Warshaw, 2002; Sindelar et al., 2002; Wendt et al., 2002). This type of mechanism was also proposed for HIV reverse transcriptase where conformational differences were observed in the positions of the catalytic carboxyl groups; however, the DNA substrate was crosslinked to the enzyme, perhaps limiting the possible enzyme structural changes that could be observed (Sarafianos et al., 2002). A second mechanism, called Brownian-ratchet motion (Astumian, 1997; Schafer et al., 1991), postulates that thermal energy in the form of Brownian motion imparts the kinetic energy to the polymerase and that the motion is biased in one direction by a device that acts like a pawl in a ratchet to prevent backtracking. NTP has been suggested to function as such a pawl for RNA polymerase by being responsible for stabilizing a translocated product primer-template (Reeder and Hawley, 1996; Komissarova and Kashlev, 1997; Nudler et al., 1997; Landick, 1997, 1998; Guajardo and Sousa, 1997; Guajardo et al., 1998). A related hypothesis suggests that the polynucleotide product of nucleotide incorporation dissociates from the RNAP product binding site (N site) and rebinds with its primer terminus in the priming site (P site); the directionality is achieved by the 3′ terminus exhibiting a higher affinity for the P site than for the N site.

Kinetic and energetic aspects of the movement of RNAP along DNA have been observed by single molecule techniques, including tethered particle visualization, optical tweezer trap studies on force generation, and observations by surface force microscopy (Yin et al., 1995; Wang et al., 1998a; Davenport et al., 2000). These studies confirm that movement along DNA follows the addition of nucleotides and implies that the polymerase converts the free energy available from nucleotide incorporation into this movement. The force generated

*Correspondence: eatherton@csb.yale.edu
[4]Present Address: Department of Chemistry and Biochemistry, University of Texas at Austin, Austin, Texas 78712.

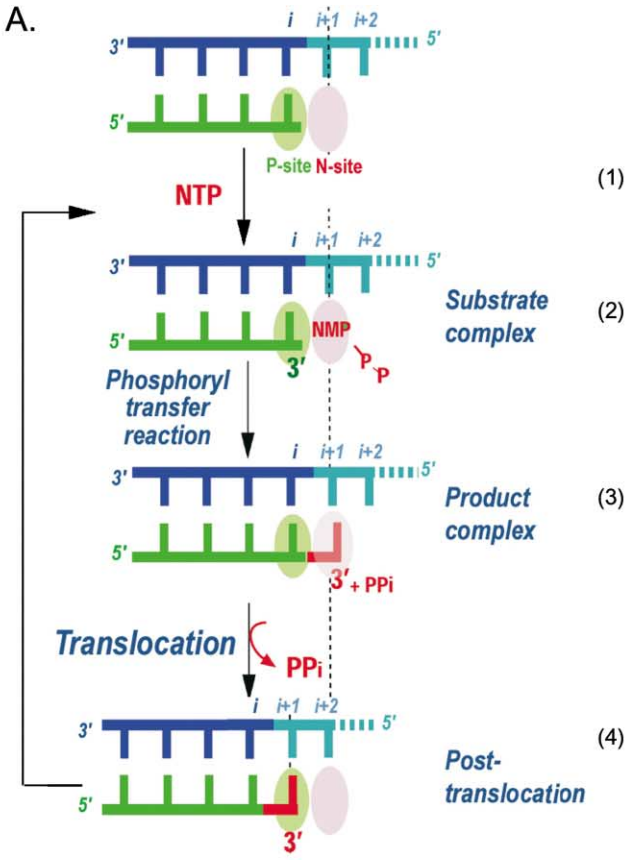

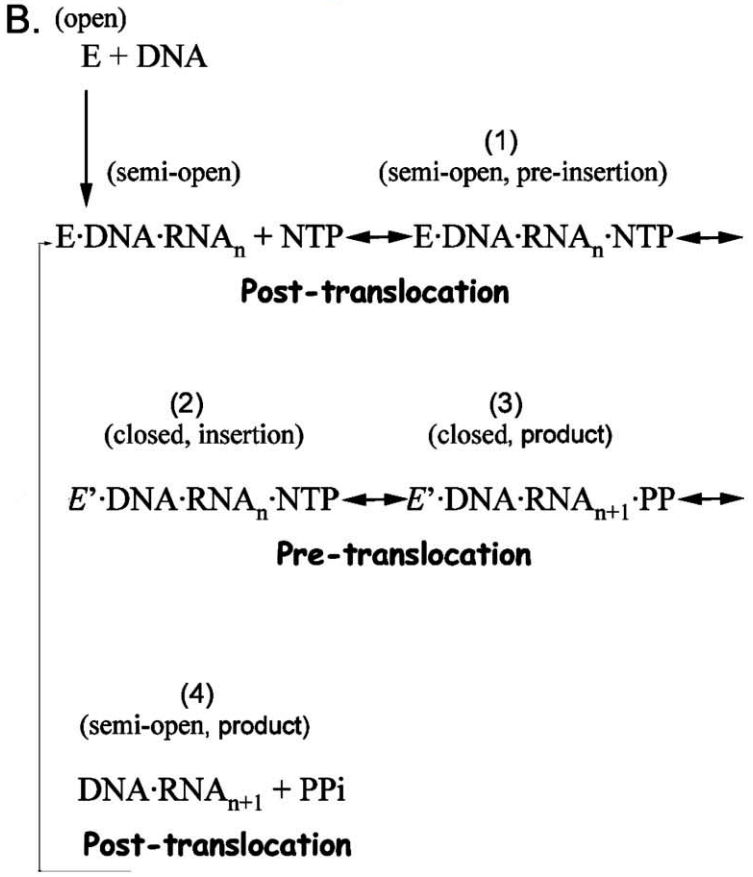

Figure 1. A Schematic Representation of a Single Nucleotide Addition Cycle

(A) (1) The cycle begins with an NTP binding to a preinsertion site (not shown) on RNAP in a posttranslocation complex.

(2) It then forms a substrate insertion complex, which contains template DNA (blue), an RNA transcript (green), and the incoming NTP (red). The template nucleotide to be transcribed (light blue) is numbered $i+1$ ($l \geq 0$). The NTP binding site is named the N site (pink), the binding site for the primer terminus of the RNA transcript is named the P site (green).

(3) The next step is the magnesium-mediated incorporation of the nucleotide onto the 3′ end of the RNA, which extends the length of the RNA by 1 nucleotide, and formation of PP_i. The newly formed 3′ primer terminus of the RNA (red) is now located in the N site.

(4) The fourth step of the reaction is the translocation of the 3′ end of the RNA transcript from the N site to the P site upon the release of PP_i.

(B) Correlation of the enzymatic reaction pathway with the structural terminology used in this paper.

upon nucleotide incorporation by RNA polymerase is approximately 15 to 20 piconewtons, which greatly exceeds the energy calculated to be required for unwinding superhelical DNA during transcription in vivo. In fact, RNAP appears to generate the largest force when compared with other well-characterized motors such as myosin and kinesin, which generate 5 to 8 piconewtons of force, respectively (Wang et al., 1998b).

Phage T7 RNA polymerase (T7 RNAP) is a single subunit RNA polymerase of about 98,000 molecular weight whose C-terminal two-thirds shows sequence and structural homology to the DNA polymerase I family of DNA polymerases (Ollis et al., 1985; Sousa et al., 1993; Jeruzalmi and Steitz, 1998; Steitz et al., 1994). The polymerase active site regions of DNA polymerase I and T7 RNAP are particularly similar, including two homologus aspartic acid residues that bind two catalytic magnesium ions and an α helix (termed the "O helix" in *E. coli* Klenow fragment) that binds the incoming dNTP and abuts the nascent base pair in a DNA polymerase ternary complex (Doublié and Ellenberger, 1998; Steitz, 1999). For clarity, we shall refer to the corresponding α helix in T7 RNA polymerase as the O helix.

Insights into the mechanism of transcription by T7 RNAP have been provided by several crystal structures, including those of initiation and elongation complexes. Comparison of the structure of a T7 RNAP initiation complex that contains promoter DNA and a 3 nucleotide RNA transcript (Cheetham and Steitz, 1999) with its structure in an elongation complex containing 30 bp of duplex DNA and a 17 nucleotide transcript shows a very large structural rearrangement of the 300 residue N-terminal domain that is unique to the RNA polymerase (Yin and Steitz, 2002; Tahirov et al., 2002). Comparison with the homologous T7 DNA polymerase, shows that both the initiation and elongation complexes are in the posttranslocation state, which is the state to which NTP is expected to bind for the next cycle of nucleotide addition. However, this RNAP conformation appeared incapable of binding NTP since the binding site for the NTP base is partially occupied by Tyr639 and the templating nucleotide i+1 is not appropriately positioned to form a base pair with an incoming nucleotide. In fact, the experiment of adding a nonhydrolyzable ATP analog to crystals of this initiation complex led to a very puzzling result. While the incoming ATP was seen to bind to this initiation complex, its base was not visible in the density map (Cheetham and Steitz, 1999). Although it was initially postulated that the incoming base competed with the tyrosine side chain for the same position, it has become clear from the results reported here that the complex being studied was of a posttranslocation product complex that can only bind the incoming nucleotide at what we term a preinsertion site.

To gain insights into NTP binding and translocation, we determined two additional crystal structures of T7 RNAP elongation complexes. One is the structure of a substrate complex containing T7 RNAP complexed with DNA having a transcription bubble, an RNA transcript, and a nonhydrolyzable ATP analog, $\alpha\beta$ methylene ATP bound at the insertion site; the other structure is that of T7 RNAP complexed with the product of nucleotide insertion and pyrophosphate (PP_i) that is in a pretranslocation state. These two new structures are in what we term a "closed" conformation that differs from a "semi-open" conformation of the posttranslocation state by

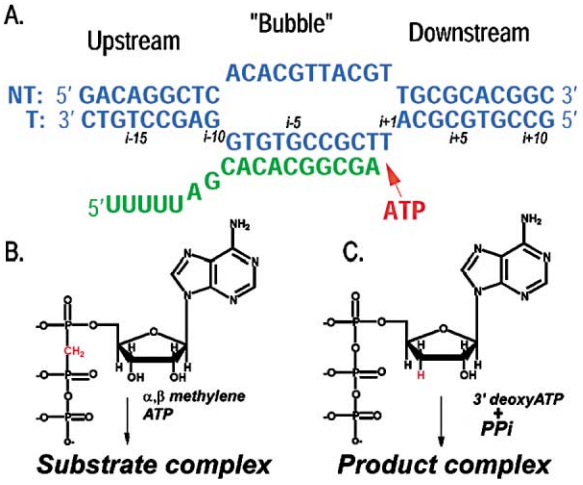

Figure 2. The Oligonucleotides and NTPs Used for Forming the Substrate and Product Complexes

(A) The transcription bubble of an elongation phase complex is mimicked by 30 bp of duplex DNA containing a central noncomplementary region; a complementary 17 nt RNA is hybridized to the template DNA in the bubble region.

(B) The substrate complex is prepared by addition of a nonhydrolyzable ATP analog, α,β methylene ATP.

(C) The product complex is formed by adding a chain terminating nucleotide, 3′ deoxyATP, as well as PP_i.

a 22° rotation of a five-helix subdomain of the fingers domain. The apo-enzyme has a conformation we term "open" since this subdomain is rotated by 45° relative to the "closed" conformation (Figure 1B). We conclude that the release of PP_i is accompanied by both translocation and downstream strand separation and stabilizes this translocated state.

Results

The two complexes of T7 RNAP whose crystal structures are described here both contained a 30 base pair duplex DNA whose central eleven nucleotides are not complementary and a 17 nucleotide RNA whose sequence at the 3′ end is complementary to the template DNA in the open bubble region (Figure 2A). The substrate complex also included a nonhydrolyzable analog of ATP, $\alpha\beta$ methylene ATP (Figure 2B), which mimics the incoming nucleotide in an elongation complex. The structure of this complex was refined at 2.88 Å resolution to an R_{fac} = 24.8% and R_{free} = 29%. Visable in the structure are 22 nt of both template and nontemplate DNA as well as 10 nt of RNA transcript and the $\alpha\beta$ methylene ATP. The second T7 RNAP structure captures the product elongation complex after the ATP has been incorporated but before the pyrophosphate product has dissociated and before the heteroduplex product has translocated. This complex was prepared by incorporating 3′ deoxyadenosine triphosphate (cordycepin) as a chain-terminating, incoming nucleotide (Figure 2C). To prevent the release of the PP_i product and to ensure the formation of the product complex, PP_i was added to the reaction mixture and the crystallization solution. The crystal structure of this product complex was determined at 2.65 Å resolution and refined to an R_{fac} = 25% and R_{free} = 28.5% (see Experimental Procedures). The relatively high R factor

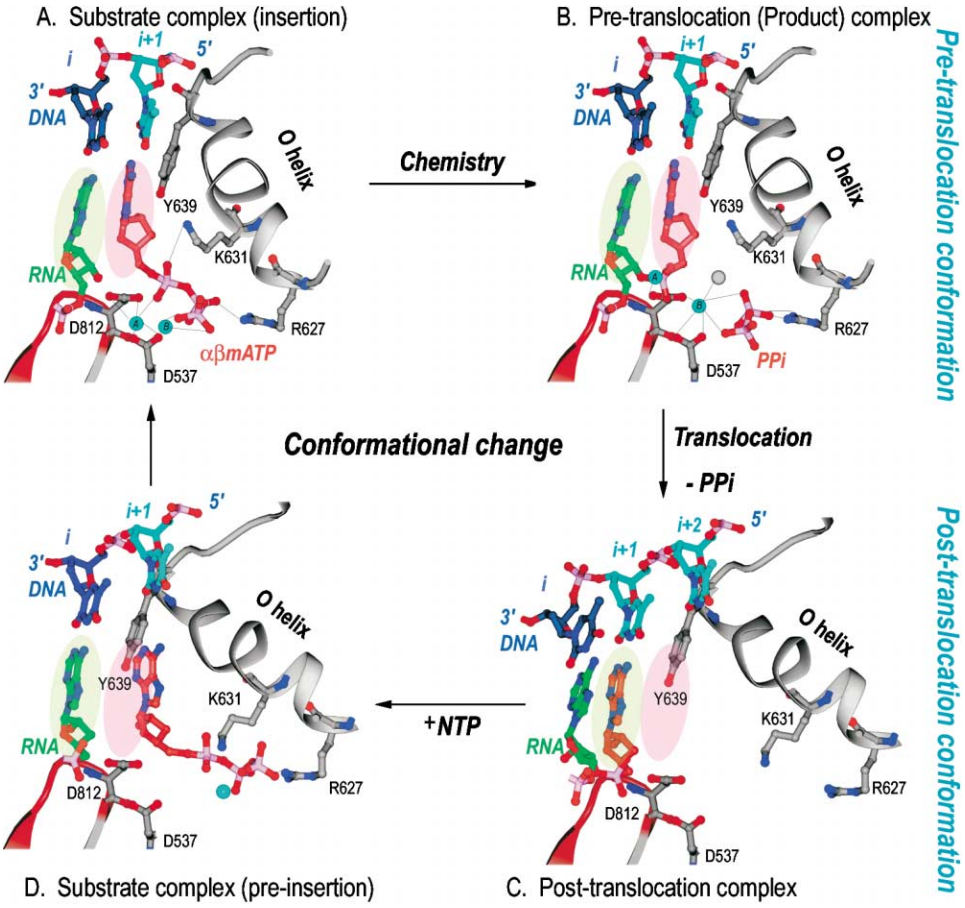

Figure 3. Structural Changes at the Active Site during a Single Nucleotide Addition Cycle

This figure shows the O helix with its phosphate binding K631 and R627, a β turn-β motif bearing the metal binding catalytic D812 and D537, template nucleotides in blue, the RNA primer terminus in green, as well as the P and N sites in green and pink ovals.

(A) The NTP (red) is bound to the N site in position to be inserted with its metal bound triphosphate moiety crosslinking the O helix to the active site aspartic acid residues. Template nucleotide i+1 (light blue) forms a base pair with the correct incoming nucleotide.

(B) The product of the phosphoryl transfer reaction shows a Mg ion (blue) bound to PP_i (red), which crosslinks D531 to R677, thereby maintaining RNAP in an identical conformation as in the substrate complex. The 3′ end of RNA remains in the N site in a pretranslocation state.

(C) Release of Mg-PP_i results in the loss of the link between the O helix and D531, which promotes the rotation of the O helix and translocation of the 3′ end of the RNA to the P site. The RNAP conformational change also places Y639 into the N site and positions the i+2 template nucleotide into the flipped-out, preinsertion position.

(D) A modeled NTP preinsertion complex with NTP bound to the posttranslocated RNAP. Although the base binding site is blocked by the side chain of Y639, the triphosphate binding site on the O helix is accessible.

may result in part from the portions of the polymerase that are disordered in the structures (residues 1–20, 230–240, 600–610). The structure shows that nucleotide incorporation has occurred, the 3′ end of the RNA has been extended by 1 nucleotide, and the product pyrophosphate is still bound to the polymerase.

Elongation Complex with Incoming NTP at the Insertion Site

The structure of an elongation complex that was formed with the nonreactive αβ methylene ATP bound to the insertion site shows the adenosine moiety of the NTP base-paired to the template nucleotide thymidine located at the i+1 position (Figure 3A). In this complex, the templating base has moved from the flipped out, preinsertion position that it occupies in the posttranslocated product complex (Yin and Steitz, 2002) to the base-pairing position seen here. The triphosphate moiety of the NTP is interacting, in part, with the positive side chains of Arg627 and Lys631 of the O helix as well as with two atoms whose location and coordination geometry are consistent with their being divalent metal ions (Figures 3A and 4A). These two presumed catalytic divalent metal ions are coordinated in turn to the catalytic aspartic acid residues 537 and 811. Metal ion A coordinates the aspartic acid carboxylates and the α phosphate of the substrate as well as the attacking 3′ OH of the RNA primer terminus while metal ion B primarily interacts with the pyrophosphate moiety of the substrate as well as the aspartic acid residues (Figure 4A). Thus it appears that the triphosphate moiety serves to electrostatically crosslink the O helix to the catalytic carboxylates via the two divalent metal ions. These simultaneous interactions between the Mg-ATP and both the basic residues of the O helix and the catalytic carboxylates are made possible by a conformational change in the fingers domain that results in the "closed" structure. The same features are seen in the structures of DNA

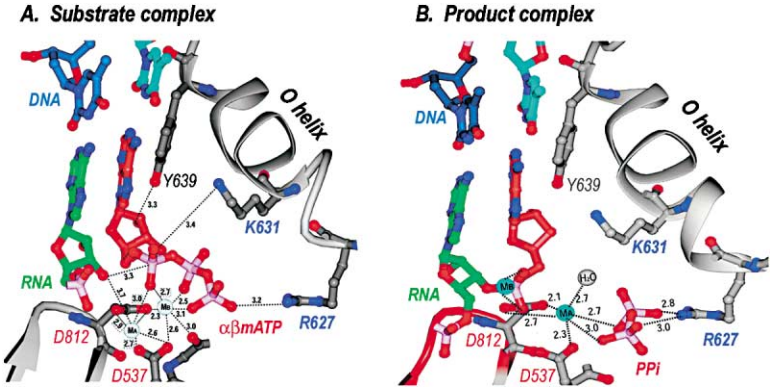

Figure 4. Detailed Interactions Made between the Incoming Substrate NTP (Red) and the Active Site before and after Incorporation at the Primer Terminus (Green)

(A) The incoming NTP is base paired with the i+1 template base (light blue). The γOH of Y639 hydrogen bonds to the 2′ OH of the NTP while K631 and R627 bind the α and γ phosphates, respectively. Two Mg ions are bound to the T7 RNAP by D812 and D537 and are also liganded to the α, β, and γ phosphates of the NTP.

(B) In the product complex, the position of the β and γ phosphates change upon forming PP_i, but are still interacting with R627 and one metal ion. The position of metal ion A has also changed.

polymerase ternary complexes (Doublié and Ellenberger, 1998).

Complex with the Product of Nucleotide Incorporation Plus Pyrophospate

The structure of the product complex shows that the 3′ dATP has been incorporated onto the 3′ end of the nascent RNA thereby extending the RNA by one nucleotide to elongate the heteroduplex from seven to eight base pairs (Figure 3B). The product PP_i remains bound in approximately the same location as the β and γ phosphates of the NTP in the substrate complex. Importantly, the PP_i is still connecting the basic residues of the O helix to a catalytic carboxylate through a divalent magnesium ion. Although two divalent metal ions are still observed in the active site, their locations have changed from those in the substrate complex. Metal ion A is associated exclusively with the 3′ end of RNA in the product complex while metal ion B remains bound to the product pyrophosphate as well as the catalytic carboxylate (Figure 4B).

T7 RNAP has the same conformation in both the incoming NTP substrate and product complexes, which indicates that the phosphoryl transfer reaction does not induce a conformational change in the enzyme nor does it promote translocation. The C_α atoms of these two structures superimpose on each other with an RMSD of 1 Å. Furthermore, the 3′ end of the RNA in the product complex and the adenosine monophosphate of the ATP in the substrate complex are both located in the N site, indicating that the product complex is in a pretranslocation state.

Posttranslocation Product Complex

The structures of the posttranslocated product complex were previously determined for both the initiation (Cheetham and Steitz, 1999) as well as the elongation phases of T7 RNA polymerase (Yin and Steitz, 2002; Tahirov et al., 2002). In both of these structures, the fingers subdomain that contains the O helix is in a semi-open conformation, and the side chain of Tyr639 is stacked on the base pair at the primer terminus. The position of this side chain in this conformation sterically blocks the base moiety of the incoming NTP from binding at the nucleotide incorporation site (N site). Furthermore, the template base in the i+1 position that is to base pair with the incoming NTP is in a "flipped out" position and located in a separate binding pocket (Figure 3C). It is not oriented in a location that would allow it to base pair with the incoming NTP even if the NTP were properly positioned for incorporation.

Preinsertion Complex with Incoming NTP

Although the incoming NTP must bind to the posttranslocation state of RNAP initially, we do not have a crystal structure of this complex in the elongation phase at this time. However, an ATP analog diffused into crystals of a posttranslocation initiation phase complex of T7 RNAP showed the analog binding to the O helix in the semi-open conformation with its adenine base poorly defined (Cheetham and Steitz, 1999). There are also crystal structures of Pol I DNA polymerase Klenow fragment complexed with deoxynucleoside triphosphate (dNTP) in the absence of primer-template DNA (Beese et al., 1993; Li et al., 1998). In these cases, the enzyme is in an "open" conformation and the dNTP is observed to interact with the O helix primarily through electrostatic interactions between the basic residues on the O helix and the phosphates of the dNTP. Thus, models of the preinsertion complex can be made by orienting an incoming NTP in a manner corresponding to the position of the dNTP in this DNA polymerase complex, consistent with the initiation phase complex (Figure 3D). Finally, a preinsertion complex with an NTP analog bound to an elongation phase complex, which is very similar to the model in Figure 3D, is described by Temiakov et al. in the accompanying paper.

Comparison of the Pretranslocation and Posttranslocation Complex Structures

The structure of T7 RNAP in the pretranslocation state was compared with its structure in the posttranslocation state by superimposing their respective palm domains, which contain the catalytic active sites. A fingers subdomain that consists of five α helices including the O helix (123 amino acids) exhibits a 22.5° rotation from its position in the "semi-open," pretranslocation product complex to that in the "closed," posttranslocation complex (Figures 5A and 5B). The fingers domain of T7 RNAP, which is composed of 218 amino acids (Thr^{566}-Glu^{785}), can be further functionally subdivided into a downstream DNA binding domain (Thr^{566}-Val^{690}) and the specificity loop (Lys^{740}-Asp^{770}), which functions to recognize the upstream promoter DNA during initiation. Only the

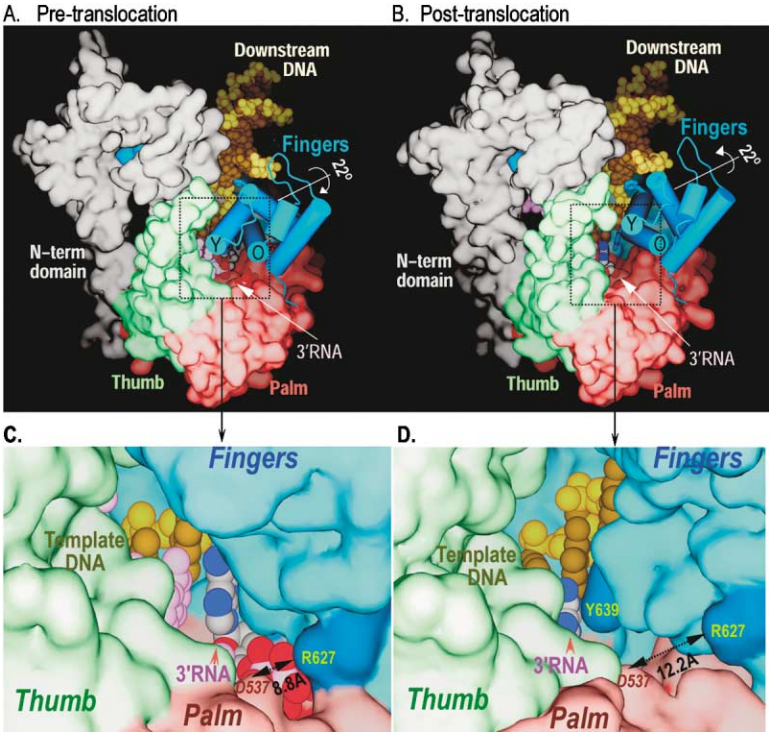

Figure 5. A Five-Helix Subdomain (Blue) of the T7 RNAP Fingers Domain, which Is Located at the Downstream Fork of the Transcription Bubble, Undergoes a 22 Degree Rotation during Translocation

The structures of pre- (A) and posttranslocation (B) complexes, which have been identically oriented by superimposing their palm domains, are shown in surface rendition, with the thumb colored green, the palm red, and the specificity loop in the fingers domain blue. Template and nontemplate DNA and RNA are colored in brown and purple, respectively. (C) and (D) are closeup views of the N site in the pre- and posttranslocation complexes, respectively. The N site is occupied by the 3′ end of the RNA transcript prior to its translocation, whereas the N site is occupied by Tyr639 after translocation. Bound PP_i (red and white) together with the metal ions bridge the basic residues of the O helix and the catalytic residue, D537, reducing the distance between D537 and R627 to 8.8 Å from the 12.2 Å in its absence.

downstream DNA binding subdomain changes its orientation during translocation.

In going from the pre- to the posttranslocation complex, the five-helix DNA binding subdomain rotates about an axis that passes through Val634 on the O helix and Gly645 on the Y helix, which is roughly parallel to the axis of the heteroduplex. The subdomain rotates about an axis that is nearly perpendicular to the heteroduplex and can act like a lever arm. The part of the domain that lies on one side of the rotation axis moves toward the primer terminus of the heteroduplex while the part of the domain on the other side moves away and appears to open up the active site. A small amino acid loop region running from the Val634 to Gly645 abuts and forms close contacts with the heteroduplex in the active site. During translocation, it moves toward the heteroduplex by 3.4 Å, the distance between base pairs in B form DNA (Figure 6). It appears that it is this pivoting movement of the helical subdomain that is responsible for translocation (Supplemental Movie S1 at http://www.cell.com/cgi/content/full/116/3/393/DC1).

The conformational change from the "semi-open" to the "closed" nucleotide insertion structure is accompanied by the movement of the templating base from the flipped out position in a pocket to a position that allows it to base pair with an incoming NTP oriented for insertion. There is also a movement of the hydroxyl group of tyrosine 639 to a location that allows it to hydrogen bond to the 2′ OH of the incoming ribose (Figures 3A and 4A); this interaction provides the structural basis for the selection of ribonucleotides over deoxyribonucleotide by the RNA polymerase, a conclusion drawn from earlier mutagenic studies (Sousa and Padilla, 1995). The binding of a deoxyribose sugar, which lacks a 2′ OH, may be less favored than that of a ribose because the tyrosine hydroxyl group would be unable to form a complementary hydrogen bond.

The pivoting rotation of the helical subdomain also changes the interactions that are made between the

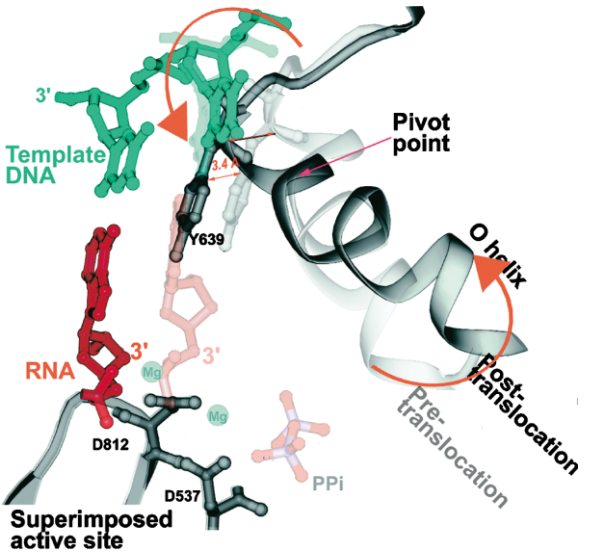

Figure 6. A Superposition of the Pre- and Posttranslocation Structures at the Active Site Showing the Pivoted Rotation Undergone by the O Helix that Is Associated with Translocation

In the pretranslocation complex (lighter colors), the O helix (light gray) is positioned in the closed conformation by PP_i (light red), which is bound to the catalytic carboxyls through Mg. In this conformation, Y639 allows formation of the new base pair (light red and blue). After PP_i release the O helix rotates around Val634, which results in the positive end of the helix moving away from the active site while the other end of the helix moves Y639 by 3.4 Å into the position of the newly formed primer terminus resulting in translocation.

incoming nucleotide bound to the O helix and the nucleotide insertion site. In the nucleotide insertion complex, which is in the fully closed conformation, the O helix interacts with both the base and the triphosphate moieties at both of its ends. The negative end of the helix dipole (Val^{634}-Ala^{638}) has a binding pocket for the base moiety while the positive end of the helix dipole (Arg^{627}-Val^{634}) binds the triphosphate moiety. The pivoting of this domain about Val634 moves the two ends of the O helix in such a way that the base site is closed and the triphosphate site is open in the posttranslocation, preinsertion state and vice versa in the insertion, pretranslocation state the base site is opened as the triphosphate site closes. The closing of the triphosphate site opens the N site for incoming NTP base binding and pairing with the i+1 template base that becomes appropriately positioned. Conversely, opening of the triphosphate site not only stabilizes the translocated state but closes the N site, which prevents backtracking of the 3′ terminus of the RNA into this site (Figure 6).

The pivoting of the helical subdomain into the closed conformation is promoted by the binding of the triphosphate moiety with its associated divalent metal ions, which allows the electrostatic crosslinking of the catalytic carboxylates to the basic residues of the O helix via these metal ions and the triphosphate. The open gap between the carboxylates and the O helix is reduced by about 3.5 Å upon NTP binding (Figures 5C and 5D). Similarly, the release of the pyrophosphate from the product complex reverses the electrostatic bridge between the O helix and the catalytic carboxylates, thereby allowing the subdomain to rotate back to the semi-open position.

While the closed conformation of the subdomain is stabilized by a phosphate-magnesium ion-mediated crosslinking of the O helix to the catalytic carboxylates, the open form appears to be stabilized by an increased interaction surface between the moving subdomain and the rest of the protein. Clearly, if the moving domain is to "spring back" from the closed to the semi-open conformation in the absence of the phosphates of NTP or pyrophosphate, there must be additional interactions that stabilize the semi-open conformation in the absence of pyrophosphate when compared with those stabilizing the closed conformation. From measurements of the solvent-accessible contact surface area of the five-helix rotating domain in both the semi-open and the closed conformations, it appears that an additional 130 $Å^2$ of the subdomain become solvent inaccessible in the semi-open, posttranslocation conformation compared with the closed, pretranslocation conformation. Assuming an energy of 25 cal/$Å^2$ of surface area buried (Chothia, 1974), the semi-open, posttranslocation conformation of the subdomain is about 3 kilocalories per mole more stable than that of the closed, pretranslocation complex in the absence of the phosphates. In contrast, the closed, pretranslocation orientation of the helical subdomain is stabilized by the electrostatic crosslinking of Mg-PP_i (or Mg-NTP), which includes two ionic hydrogen bonds between the O helix and PP_i and two bonds between Mg^{2+} and the catalytic carboxylate. While electrostatic stabilization free energy is difficult to estimate, the closed conformation could be stabilized by as much as 6 to 8 Kcal/mole by Mg-PP_i (assuming 2 to 3 Kcal/mole per ionic bond), making it 3 to 5 Kcal/mole more stable than the semi-open conformation in the presence of Mg-NTP or Mg-PP_i, which agrees well with thermodynamic measurements (Astatke et al., 1995; Sousa et al., 1992). These very approximate energy calculations are consistent with the observation that T7 RNAP is in the closed, pretranslocation conformation in the presence of Mg-PP_i (or Mg-NTP) and in the open conformation in its absence.

It should be noted that the pretranslocation and posttranslocation complexes are packed identically in crystals that are isomorphous. In both structures, the fingers domain is not involved in any crystal contacts. Therefore, the conformational changes of the fingers domain that are observed between the pre- and posttranslocation crystal structures are not influenced by crystal packing, but rather reflect the stable conformations of the different states of ligation.

Strand Displacement, Helicase Mechanism

Comparison of the pre- and posttranslocation complex structures shows that the fingers subdomain rotation resulting from PP_i dissociation is associated with the unwinding of the downstream duplex DNA by one base pair concomitant with translocation (Figure 7 and Supplemental Movie S2 on *Cell* website). As the domain rotation results in the primer terminus of the heteroduplex product moving from the nucleotide insertion site (N site) to the primer terminus site (P site), the downstream template strand is necessarily also translocated by 3.4 Å. As described previously (Yin and Steitz, 2002), the Y helix in the helical subdomain of the fingers domain lies at the junction between the downstream template and nontemplate strands where they become separated (Helix Y is helix P in DNAP I and follows helix "O"). The pivot axis about which the subdomain rotates passes through Gly645 on the Y helix, adjacent to Phe644 which is located at the duplex fork. The pivoting of the subdomain around Gly645 does not significantly change the stacking interaction that is possible between Phe644 and the next base of the template nucleotide after translocation (Figure 7).

The translocation step is also accompanied by the displacement of one RNA transcript nucleotide from the template strand. Analogous to the unwinding of the downstream duplex, the separation of the RNA from the template strand is accomplished by an α helix in the thumb domain that lies in the fork between the RNA and template DNA at the point of their separation (Yin and Steitz, 2002). During the translocation step, one DNA-DNA base pair and one DNA-RNA base pair are broken and one DNA-DNA base pair is formed at the upstream end of the transcription bubble for a net change of one base pair broken. Again, the energy and direction for this change appear to be derived from the incoming NTP, expressed at the step of pyrophosphate dissociation.

Discussion

The structures of T7 RNAP substrate and product complexes reported here, along with the previously determined structure of T7 RNAP bound to a posttranslocated product, represent three of the four structural states of the nucleotide incorporation cycle (Figures 1B and 3) of RNA polymerase. The fourth state, that of a substrate complex with the incoming nucleotide bound to a prein-

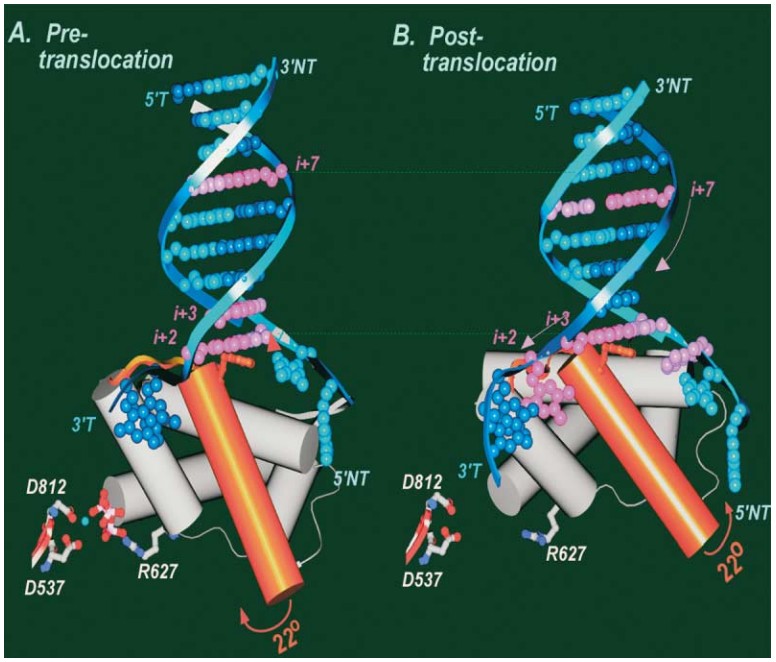

Figure 7. Rotation of the Five-Helix Moving Part (Represented by Cylinders) Results in Translocation of the Heteroduplex Product

This helical subdomain is located at the downstream fork of the transcription bubble and undergoes a 22 degree rotation between the pretranslocation (A) and posttranslocation (B) states. Downstream DNA is colored in blue with base pairs i+2, i+3, and i+7 colored in purple to highlight translocation. During translocation, the 5 helix bundle separates the downstream DNA at the i+2 base pair. The Y helix (orange) lies at this junction and F644 stacks on the i+2 base pair in the pretranslocation state and the i+3 base pair in the posttranslocation state. The ionic link between R627 and D537 provided by PP_i in the pretranslocation state is lost by the 22 degree rotation to the posttranslocation state.

sertion site, is described in detail in an accompanying paper (Temiakov et al., 2004 [this issue of *Cell*]) and was seen previously in an initiation complex whose polymerase domain conformation is the same as that of the posttranslocation elongation complex (Cheetham and Steitz, 1999). The major observations are that a five α helix subdomain of the fingers domain that includes the O helix assumes two conformational states in the incorporation cycle; the transition to the "semi-open" conformation is promoted by pyrophosphate dissociation and is correlated with translocation of the heteroduplex product as well as strand separation of the downstream DNA duplex (Supplemental Movies S1 and S2 on *Cell* website).

Three related conformations of the fingers domain of T7 RNAP have now been observed, which we refer to as "open," "semi-open," and "closed" (Figure 8). Superposition of palm domains of the apo-T7 RNAP (Chen et al., 1999; Jeruzalmi and Steitz, 1998), the posttranslocation complex (Cheetham and Steitz, 1999; Tahirov et al., 2002; Yin and Steitz, 2002), and the pretranslocation complex shows that the apo-enzyme has its fingers helical subdomain in the most open conformation. When the RNAP apo-enzyme first associates with the promoter DNA, it undergoes a well-documented "closing" structural transition between the fingers and the palm domains that has been observed previously in DNA polymerases. The complex with the promoter DNA alone (Cheetham et al., 1999) has the enzyme conformation of the posttranslocation complex that we are now terming "semi-open." It is about 23° more closed than the apo-enzyme. This initial 23° swing in the fingers domain is distinct from the 22° rotation that relates the structures of T7 RNAP in the pre- and posttranslocation complexes (Figure 8). The initial open to semi-open conformational change occurs only once at the beginning of transcription while the conformational changes between the pre- and posttranslocation stages described above occur at every cycle of nucleotide addition.

The "closed" state allows the corrected positioning of an incoming NTP for its incorporation and corresponds to the "closed" structure observed in the ternary complexes of DNA polymerases. Likewise, the complex with the product of nucleotide incorporation including pyrophosphate is observed in this same, closed conformational state. The transition to the other conformational state, which we term a "semi-open" state, is accompanied by the translocation of the duplex product as well as the strand separation of downstream duplex DNA (Figures 5A and 5B). This semi-open conformation

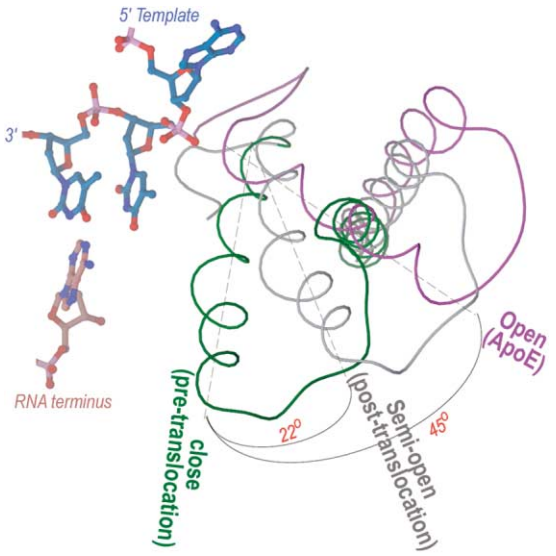

Figure 8. The Relative Orientation of the Fingers Helical Subdomain in the Apo-T7 RNAP ("Open" Conformation, Purple), the Posttranslocation ("Semi-Open" Conformation, Gray), and Pretranslocation ("Closed" Conformation, Green)

Only two helices of the subdomain are shown. The axis of the O helix rotates by 45° between two open and closed structures and by 22° between the semi-open and closed structures. The template strand (blue) and primer terminus (gray) are shown in the posttranslocation position.

of T7 RNAP corresponds to the "open" structures of apo- and binary primer-template DNA complexes of DNA polymerases, which also undergo the transition to a similar closed conformation (Doublié and Ellenberger, 1998).

Two functional roles for the observed NTP (or dNTP) induced conformational changes in the fingers domain of DNA and RNA polymerases have been advanced. First, Ellenberger, Kraut and coworkers (Doublié and Ellenberger, 1998; Pelletier et al., 1996) have suggested that this nucleotide-induced change plays a very significant role in increasing the fidelity of nucleotide incorporation. From the structures of ternary complexes of T7 DNA polymerase and DNA polymerase β, they have each suggested that only a correct Watson Crick base pair will fit into the pocket that is formed surrounding the nascent base pair and thus allow the conformational change that is necessary to correctly position the nascent nucleotide for catalysis of insertion. An incorrect incoming nucleotide forming a noncanonical base pair that lacks a complementary interaction with the enzyme will dissociate prior to the chemical step, consistent with kinetic studies (Dahlberg and Benkovic, 1991). Structural studies of other Pol I enzymes (Johnson et al., 2003; Kiefer et al., 1998), reverse transcriptase (Huang et al., 1998), and B family RB69 DNA polymerase (Wang et al., 1997; Shamoo and Steitz, 1999; Franklin et al., 2001) are also consistent with this role for the conformational change.

Beese and coworkers (Johnson et al., 2003) have added a second role for the NTP-induced conformational change in DNA polymerase. They propose that the conformational changes are coupled to prevention of frame shifts that may result in deletions. While this manuscript was in preparation, they published the structure of *B. stearothermophilus* Pol I large fragment DNA polymerase ternary complex (Johnson et al., 2003), which when compared with their previously determined structure of a binary complex showed similar fingers domain and substrate conformational changes to those presented here. The flipped-out position of the i+1 templating base in the preinsertion pocket can prevent template strand slippage, which could lead to deletions within the copied DNA (Johnson et al., 2003).

Pyrophosphate Dissociation and Translocation

We suggest here that there are two additional important functional roles for the fingers conformational changes associated with NTP binding and PP_i dissociation—powering duplex product translocation and downstream duplex strand separation. The binding of NTP (dNTP) leads to the closing conformational change that appears to be coupled to correct incoming nucleotide selection as described above. It is the reversal of this conformational change, promoted by PP_i dissociation, that is associated with translocation and strand displacement. This conclusion that dissociation of PP_i is driving translocation and stand separation appears valid because the only difference between the isomorphous crystals of the pre- and posttranslocation states is the presence or absence of PP_i. Although the structure of a DNA Pol I product complex with PP_i is unknown, the same mechanism of translocation and strand separation proposed for RNAP appears likely in the Pol I family DNA polymerases since the same conformational change in the fingers domain of *B. subtilus* DNA Pol I is observed between a posttranslocation DNAP-DNA binary complex and the DNAP-DNA-dNTP ternary complex (Kiefer et al., 1998; Johnson et al., 2003). Furthermore, the conclusion that translocation and strand displacement (where it occurs) are driven by PP_i dissociation appears plausible for all polymerases exhibiting a nucleotide-induced conformational change, even though the structures of DNA polymerases (or multisubunit RNA polymerases) associated with all four incorporation states are not known.

An exception to our proposed mechanism of translation may be provided by the family of DNA lesion bypass DNA polymerases, which replicate regions of damaged DNA, often with low fidelity and processivity (Boudsocq et al., 2002; Goodman, 2002; Marx and Summerer, 2002). It appears that these polymerases do not undergo the dNTP-induced conformational change exhibited by other families of DNA polymerases. The first structure of a bypass polymerase, a fragment of a DinB homolog without any bound ligands, exhibited a fingers conformation that was in the closed state, when compared with the structures of ternary complexes of other DNA polymerase family enzymes (Zhou et al., 2001). Indeed, the subsequent cocrystal structure of a related lesion bypass polymerase complexed with DNA and dNTP (Ling et al., 2001) had a virtually identical closed conformation as that of the apo-enzyme. It is possible that the low processivity, lack of strand displacement activity, and ability to bypass nonstandard bases in the template strand are related to the apparent lack of any dNTP- or PP_i-induced conformational changes. In this case, translocation may result from product dissociation from the N site and its rebinding with its 3′ terminus at the P site.

An alternative mechanism that has been proposed for RNAP translocation, the Brownian ratchet mechanism, differs from the power stroke proposal with respect to the source of the energy for movement and the manner in which that energy can be used to bias movement in one direction. In this mechanism, the RNAP can slide and oscillate between the pre- and posttranslocation states driven by the thermal energy of Brownian motion of all neighboring molecules. The motion in one dimension is biased in one direction by means of a pawl device that prevents backsliding of the polymerase as it ratchets along the DNA. NTP is envisioned to act as a pawl and to intermittently block the backsliding of the heteroduplex. It is the binding of NTP that is proposed to drive translocation by preventing the rebinding of the 3′ terminus of the primer strand in the N site (Reeder and Hawley, 1996; Komissarova and Kashlev, 1997; Nudler et al., 1997; Landick, 1997, 1998; Guajardo et al., 1998). That is not what we and Temiakov et al. (2004 [this issue of *Cell*]) observe. NTP binds to the posttranslocation state that is already stabilized by the semi-open conformation. The DNA substrate may, of course, diffuse in one dimension along the polymerase active site and in the case of DNA polymerases can move to the exonuclease domain for editing. However, it is the conformational state of the enzyme that dictates whether the most stable equilibrium position of the 3′ terminus, the primer strand, is in the pretranslocation position, the N site, or in the posttranslocation position, the P site. After the dissociation of PP_i and the associ-

ated rotation of the five-helix subdomain, only the P site is accessible for binding the primer terminus. Thus, in contrast to the Brownian ratchet model for translocation, we propose, based on these structures, that it is the PP_i-driven conformational change in the fingers domain that prevents the 3′ terminus from binding in the N site, not the binding of NTP. Whether the helical domain rotation produced by PP_i dissociation "pushes" the heteroduplex to the P site or blocks access of a rapidly diffusing heteroduplex to the N site depends on the relative rates of the conformational change and heteroduplex dissociation, which are currently unknown.

Other Motor Molecules and Cellular RNA Polymerases

Other molecular mechanical systems, including myosin-actin contraction in muscle and F_1-ATP synthase in mitochondria, appear to work in an analogous way. These are ATPases or GTPases and it is the dissociation of the product phosphate that promotes the enzyme conformational changes that are coupled to mechanical movement, e.g., power stroke in muscle contraction and rotary motion of F_1-ATP synthase for ATP synthesis, unwinding of DNA or RNA by helicases (Oster and Wang, 2003; Vale and Milligan, 2000; Warnock and Schmid, 1996; Yeagle and Albert, 2003). Likewise, the complete conversion of the ATP or GTP to ADP or GDP plus phosphate does not trigger the conformational change. It is the dissociation of P_i that is associated with the conformational change in the enzyme and expresses the work of the process.

As with T7 RNAP, the multisubunit cellular DNA-dependent RNA polymerases translocate down the template processively after each nucleotide incorporation while opening the downstream duplex and peeling off the RNA transcript. However, the mechanism by which this process is coupled to NTP incorporation is not clear. Based on the structures of a yeast RNA Pol II elongation complex in the pretranslocation complex (Gnatt et al., 2001) and a *Thermus aquaticus* RNAP apo-enzyme (Zhang et al., 1999), it has been suggested that translocation is promoted by a structural transition in the "bridging" helix, whose location and orientation relative to the primer terminus is similar to that of the O helix in T7 RNAP. In the bacterial apo-enzyme, the bridge helix has a bend that bulges near its middle while in the yeast Pol II it is more nearly straight. Unfortunately, the structures of all of the appropriate complexes for understanding translocation are currently not available since neither the structure of the posttranslocation complex nor the structures that include the incoming NTP or PP_i are known. While the bacterial apo-enzyme structure might or might not correspond to the posttranslocation enzyme conformation as proposed, there is currently no information on how the binding and dissociation of the β and α phosphates of NTP or the product PP_i might be coupled to an enzyme conformational transition analogous to what occurs in T7 RNAP. Presumably, the binding of NTP and the dissociation of PP_i promote the conformational transitions between pre- and post-translocation mediated by Mg-phosphate interactions, although the actual conformational alterations are most likely different than those observed with T7 RNAP.

Energetic Considerations

How should one most appropriately understand the mechanism by which the energy contained in the NTP molecules being incorporated is coupled to translocation of the heteroduplex product and the associated enzyme conformational changes? Since there are no significant structural changes in the polymerase upon formation of the product heteroduplex plus PP_i from the substrates, the high energy of NTP is not expressed in translocation or strand separation at that step. The high energy state of NTP is expressed in two chemical steps: first, the phosphoryl transfer reaction resulting in nucleotide addition and formation of pyrophosphate; second, the pyrophosphatase-catalyzed hydrolysis of the PP_i product to P_i. In both cases, the high energy states of NTP and PP_i assure that the respective chemical reactions go to completion. The enzyme conformational changes that are necessary for fidelity, translocation, and helicase activities are generated by NTP binding and by pyrophosphate release. Phosphodiester bond formation does not contribute to any change in enzyme conformation. Rather, the complete conversion of NTP to PP_i and the subsequent release of PP_i generates the power stroke conformational change resulting in translocation. Since the cellular concentration of pyrophosphate in *E. coli* is constant at 0.5 microM (Kukko, 1982; Kukko-Kalske et al., 1989) and the apparent Kd for PP_i for T7RNRAP is 0.83 microM (Guajardo and Sousa, 1997), pyrophosphate release is favored.

In summary, strand separation and translocation by T7 RNA polymerase appear to be affected by a power stroke mechanism in which the dissociation of Mg PP_i promotes the relevant enzyme conformational change. An element of a ratchet mechanism may be provided by Tyr639 and by the binding pocket for the flipped out i+1 template base in the posttranslocation state. This binding site may present an energy barrier to slippage or backsliding that can be overcome by the binding of an NTP whose base is complementary to the i+1 template base.

Experimental Procedures

Preparation and Crystallization of T7 RNAP Substrate and Product Complexes

The plasmid containing the T7 RNAP gene (p2119) was cloned into BL21 cells. T7 RNAP was purified according to the previously published protocol (Jeruzalmi and Steitz, 1998).

The scaffold that mimics the transcription bubble was formed by three strands of oligonucleotides. Oligonucleotides that represent template DNA (3′ CTGTCCTAGGTGTGCCGCTTACGCGTGCCG) and nontemplate DNA (5′GACAGGCTCACACGTTACGTTGCGCACGCG3′) were synthesized by the Keck facility at Yale University and purified by reversed phase HPLC. The RNA oligonucleotide (5′UUUUUAG CACACGGCGA3′) was purchased from Dharmacon Inc. and purified on a denaturing polyacrylimide gel (20%). The transcription bubble was assembled by mixing the template and nontemplate DNA with RNA at a 1:1:1.2 molar ratio. The mixture was incubated at 75°C for 5 min in a solution containing Tris-HCl (50 μM, pH 7.5), NaCl (20 μM), and magnesium acetate (10 μM) and was then allowed to cool to 20°C during the course of 2 hr. The substrate complex was formed by incubating T7 RNAP (200 μM), the transcription bubble (200 μM), and $\alpha\beta$ methylene ATP (1 μM) in the solution described above at 37°C for 5 min. The substrate complex was crystallized under the conditions Tris-HCl (50 μM, pH 7.4), PEG8000 (6%), Li_2SO_4 (200 μM), Mg acetate (10 μM), and DTT (10 μM) at 21°C by the vapor diffusion method. The product complex was formed by incubating T7 RNAP

(200 μM), the transcription bubble (200 μM), 3′deoxyadenosine triphosphate (cordacipin), and pyrophosphate (200 μM) at 37°C for 5 min to ensure completion of the enzymatic reaction. The product complex crystals were obtained under the conditions of Tris-HCl (50 mM, pH 7.0), PEG8000 (8%), Li_2SO_4 (200 mM), Mg acetate (10 mM), and DTT (10 mM) at 21°C. The crystal trays were kept under a non-oxidizing environment using argon gas. Crystals were stabilized in a higher concentration of precipitant (12% PEG 8K) and in glycerol (25%, v/v) for 5–10 min prior to their cryofreezing.

Structure Determination

The diffraction data from crystals of the pretranslocation product complex including PP_i were collected to 2.65 Å resolution at the Cornell High Energy Synchrotron Source (CHESS), A1 beamline. The crystals are in space group $C222_1$ with unit cell dimensions a = 137 Å, b = 145 Å, c = 141 Å, $\alpha = \beta = \gamma = 90°$. These crystals are very similar to the crystals of the posttranslocation product complex whose structure was previously determined (Yin and Steitz, 2002); these crystals are in space group $C222_1$ with unit cell dimensions a = 142.9, b = 145.5, and c = 145.6. The structure of the new complex was determined by the molecular replacement method using the previous structure of the T7 RNAP elongation complex as a search model (Brünger et al., 1998; Navaza, 2001). The rotation and translation search results showed an unambiguous solution. Even at this initial stage, the difference Fourier map (Fo-Fc, ϕ_{MR}) revealed a clearly different conformation of the fingers domain as compared to the posttranslocation model. The structure was subsequently refined by rigid-body refinement, energy minimization, simulated-annealing, and B factor refinement (Brünger et al., 1998). The final model has an R factor = 25% and Rfree = 28.5%.

Diffraction data from the crystals of the substrate complex including the incoming NTP were collected to 2.88 Å resolution at the Advance Photo Source (APS),19-ID beamline. The crystals are in space group $C222_1$, with unit cell dimensions of a = 138 Å, b = 145 Å, c = 146 Å, $\alpha = \beta = \gamma = 90°$, nearly isomorphous with the posttranslocated product complex. The structure was determined by the molecular replacement method using both pretranslocation and posttranslocation complex as search models. The solution from using the pretranslocation complex as a search model gave rise to higher rotation and translocation function peaks than that from using the posttranslocation complex model. The correlation coefficient was 51% with the pretranslocation complex and 44% with the posttranslocation complex, suggesting that the structure of the substrate complex was closely related to that of the pretranslocation complex. The model was refined to an R factor = 24.8%, Rfree = 29%.

The atomic coordinates for the T7 RNAP substrate and product complexes reported here, as well as the corresponding experimental diffraction amplitudes have been deposited in the Protein Data Bank with accession numbers 1s76 and 1s77.

Acknowledgments

This research was supported by a National Institutes of Health grant GM57510 to T.A.S. We thank Cathy Joyce and William Kennedy for insightful comments on the manuscript. X-ray data were collected at the Cornell High Energy Synchrotron Source (CHESS), MacCHESS beamline A1 and at the Argonne Advanced Photon Source beamline 19-ID. We wish to thank the staff at these synchrotron facilities for their assistance in data collection.

Received: September 15, 2003
Revised: December 18, 2003
Accepted: January 14, 2004
Published: February 5, 2004

References

Astatke, M., Grindley, N.D., and Joyce, C.M. (1995). Deoxynucleoside triphosphate and pyrophosphate binding sites in the catalytically competent ternary complex for the polymerase reaction catalyzed by DNA polymerase I (Klenow fragment). J. Biol. Chem. *270*, 1945–1954.

Astumian, R.D. (1997). Thermodynamics and kinetics of a Brownian motor. Science *276*, 917–922.

Beese, L.S., Friedman, J.M., and Steitz, T.A. (1993). Crystal structures of the Klenow fragment of DNA polymerase I complexed with deoxynucleoside triphosphate and pyrophosphate. Biochemistry *32*, 14095–14101.

Boudsocq, F., Ling, H., Yang, W., and Woodgate, R. (2002). Structure-based interpretation of missense mutations in Y-family DNA polymerases and their implications for polymerase function and lesion bypass. DNA Repair (Amst.) *1*, 343–358.

Brünger, A.T., Adams, P.D., Clore, G.M., DeLano, W.L., Gros, P., Grosse-Kunstleve, R.W., Jiang, J.S., Kuszewski, J., Nilges, M., Pannu, N.S., et al. (1998). Crystallography & NMR system: A new software suite for macromolecular structure determination. Acta Crystallogr. D Biol. Crystallogr. *54*, 905–921.

Cheetham, G.M., and Steitz, T.A. (1999). Structure of a transcribing T7 RNA polymerase initiation complex. Science *286*, 2305–2309.

Cheetham, G.M., Jeruzalmi, D., and Steitz, T.A. (1999). Structural basis for initiation of transcription from an RNA polymerase-promoter complex. Nature *399*, 80–83.

Chen, C.J., Liu, Z.J., Rose, J.P., and Wang, B.C. (1999). Low-salt crystallization of T7 RNA polymerase: a first step towards the transcription bubble complex. Acta Crystallogr. D Biol. Crystallogr. *55*, 1188–1192.

Chothia, C. (1974). Hydrophobic bonding and accessible surface area in proteins. Nature *248*, 338–339.

Dahlberg, M.E., and Benkovic, S.J. (1991). Kinetic mechanism of DNA polymerase I (Klenow fragment): identification of a second conformational change and evaluation of the internal equilibrium constant. Biochemistry *30*, 4835–4843.

Davenport, R.J., Wuite, G.J., Landick, R., and Bustamante, C. (2000). Single-molecule study of transcriptional pausing and arrest by E. coli RNA polymerase. Science *287*, 2497–2500.

Dedrick, R.L., Kane, C.M., and Chamberlin, M.J. (1987). Purified RNA polymerase II recognizes specific termination sites during transcription in vitro. J. Biol. Chem. *262*, 9098–9108.

Doublié, S., and Ellenberger, T. (1998). The mechanism of action of T7 DNA polymerase. Curr. Opin. Struct. Biol. *8*, 704–712.

Franklin, M.C., Wang, J., and Steitz, T.A. (2001). Structure of the replicating complex of a pol alpha family DNA polymerase. Cell *105*, 657–667.

Gnatt, A.L., Cramer, P., Fu, J., Bushnell, D.A., and Kornberg, R.D. (2001). Structural basis of transcription: an RNA polymerase II elongation complex at 3.3 A resolution. Science *292*, 1876–1882.

Goodman, M.F. (2002). Error-prone repair DNA polymerases in prokaryotes and eukaryotes. Annu. Rev. Biochem. *71*, 17–50.

Guajardo, R., and Sousa, R. (1997). A model for the mechanism of polymerase translocation. J. Mol. Biol. *265*, 8–19.

Guajardo, R., Lopez, P., Dreyfus, M., and Sousa, R. (1998). NTP concentration effects on initial transcription by T7 RNAP indicate that translocation occurs through passive sliding and reveal that divergent promoters have distinct NTP concentration requirements for productive initiation. J. Mol. Biol. *281*, 777–792.

Huang, J., and Sousa, R. (2000). T7 RNA polymerase elongation complex structure and movement. J. Mol. Biol. *303*, 347–358.

Huang, H., Chopra, R., Verdine, G.L., and Harrison, S.C. (1998). Structure of a covalently trapped catalytic complex of HIV-1 reverse transcriptase: implications for drug resistance. Science *282*, 1669–1675.

Ikeda, R.A., and Richardson, C.C. (1986). Interactions of the RNA polymerase of bacteriophage T7 with its promoter during binding and initiation of transcription. Proc. Natl. Acad. Sci. USA *83*, 3614–3618.

Jeruzalmi, D., and Steitz, T.A. (1998). Structure of T7 RNA polymerase complexed to the transcriptional inhibitor T7 lysozyme. EMBO J. *17*, 4101–4113.

Jiang, M.Y., and Sheetz, M.P. (1994). Mechanics of myosin motor: force and step size. Bioessays *16*, 531–532.

Johnson, S.J., Taylor, J.S., and Beese, L.S. (2003). Processive DNA synthesis observed in a polymerase crystal suggests a mechanism for the prevention of frameshift mutations. Proc. Natl. Acad. Sci. USA *100*, 3895–3900.

Kiefer, J.R., Mao, C., Braman, J.C., and Beese, L.S. (1998). Visualizing DNA replication in a catalytically active Bacillus DNA polymerase crystal. Nature *391*, 304–307.

Komissarova, N., and Kashlev, M. (1997). RNA polymerase switches between inactivated and activated state by translocating back and forth along the DNA and the RNA. J. Biol. Chem. *272*, 15329–15338.

Krakow, J.S., and Fronk, E. (1969). Azotobacter vinelandii ribonucleic acid polymerase. 8. Pyrophosphate exchange. J. Biol. Chem. *244*, 5988–5993.

Kuhko, E., and Heinonen, J. (1986) The intracellular concentration of pyrophosphate in the batch culture of Escherichia coli. Eur. J. Biochem. *127*, 347–349.

Kukko-Kalske, E., Lintunen, M., Inen, M.K., Laht, R., and Heinonen, J. (1989). Intracellular PPi concentration is not directly dependent on amount of inorganic pyrophosphatase in Escherichia coli K-12 cells. J. Bacteriol. *171*, 4498–4500.

Landick, R. (1997). RNA polymerase slides home: pause and termination site recognition. Cell *88*, 741–744.

Landick, R. (1998). RNA polymerase as a molecular motor. Cell *93*, 13–16.

Li, Y., Kong, Y., Korolev, S., and Waksman, G. (1998). Crystal structures of the Klenow fragment of *Thermus aquaticus* DNA polymerase I complexed with deoxyribonucleoside triphosphate. Protein Sci. *7*, 1116–1123.

Ling, H., Boudsocq, F., Woodgate, R., and Yang, W. (2001). Crystal structure of a Y-family DNA polymerase in action: a mechanism for error-prone and lesion-bypass replication. Cell *107*, 91–102.

Lorch, Y., LaPointe, J.W., and Kornberg, R.D. (1987). Nucelosomes inhibit the initiation of transcription but allow chain elongation with the displacement of histone. Cell *49*, 203–210.

Martin, C.T., Muller, D.K., and Coleman, J.E. (1988). Processivity in early stages of transcription by T7 RNA polymerase. Biochemistry *27*, 3966–3974.

Marx, A., and Summerer, D. (2002). Molecular insights into error-prone DNA replication and error-free lesion bypass. Chembiochem. *3*, 405–407.

Navaza, J. (2001). Implementation of molecular replacement in AMoRe. Acta Crystallogr. D Biol. Crystallogr. *57*, 1367–1372.

Nudler, E., Mustaev, A., Lukhtanov, E., and Goldfarb, A. (1997). The RNA-DNA hybrid maintains the register of transcription by preventing backtracking of RNA polymerase. Cell *89*, 33–41.

Ollis, D.L., Brick, P., Hamlin, R., Xuong, N.G., and Steitz, T.A. (1985). Structure of large fragment of Escherichia coli DNA polymerase I complexed with dTMP. Nature *313*, 762–766.

Oster, G., and Wang, H. (2003). Rotary protein motors. Trends Cell Biol. *13*, 114–121.

Pelletier, H., Sawaya, M.R., Wolfle, W., Wilson, S.H., and Kraut, J. (1996). Crystal structures of human DNA polymerase beta complexed with DNA: implications for catalytic mechanism, processivity, and fidelity. Biochemistry *35*, 12742–12761.

Reeder, T.C., and Hawley, D.K. (1996). Promoter proximal sequences modulate RNA polymerase II elongation by a novel mechanism. Cell *87*, 767–777.

Reedy, M.C. (2000). Visualizing myosin's power stroke in muscle contraction. J. Cell Sci. *113*, 3551–3562.

Sarafianos, S.G., Clark, A.D., Jr., Das, K., Tuske, S., Birktoft, J.J., Ilankumaran, P., Ramesha, A.R., Sayer, J.M., Jerina, D.M., Boyer, P.L., et al. (2002). Structures of HIV-1 reverse transcriptase with pre- and post-translocation AZTMP-terminated DNA. EMBO J. *21*, 6614–6624.

Schafer, D.A., Gelles, J., Sheetz, M.P., and Landick, R. (1991). Transcription by single molecules of RNA polymerase observed by light microscopy. Nature *352*, 444–448.

Shamoo, Y., and Steitz, T.A. (1999). Building a replisome from interacting pieces: sliding clamp complexed to a peptide from DNA polymerase and a polymerase editing complex. Cell *99*, 155–166.

Sindelar, C.V., Budny, M.J., Rice, S., Naber, N., Fletterick, R., and Cooke, R. (2002). Two conformations in the human kinesin power stroke defined by X-ray crystallography and EPR spectroscopy. Nat. Struct. Biol. *9*, 844–848.

Sousa, R. and Padilla, R. (1995). A mutant T7 RNA polymerase as a DNA polymerase. EMBO J. *14*, 4609–4621.

Sousa, R., Patra, D., and Lafer, E.M. (1992). Model for the mechanism of bacteriophage T7 RNAP transcription initiation and termination. J. Mol. Biol. *224*, 319–334.

Sousa, R., Chung, Y.J., Rose, J.P., and Wang, B.C. (1993). Crystal structure of bacteriophage T7 RNA polymerase at 3.3 Å resolution. Nature *364*, 593–599.

Steitz, T.A. (1999). DNA polymerases: structural diversity and common mechanisms. J. Biol. Chem. *274*, 17395–17398.

Steitz, T.A., Smerdon, S.J., Jäger, J., and Joyce, C.M. (1994). A unified polymerase mechanism for nonhomologous DNA and RNA polymerases. Science *266*, 2022–2025.

Tahirov, T.H., Temiakov, D., Anikin, M., Patlan, V., McAllister, W.T., Vassylyev, D.G., and Yokoyama, S. (2002). Structure of a T7 RNA polymerase elongation complex at 2.9 A resolution. Nature *420*, 43–50.

Temiakov, D., Patlan, V., Anikin, M., McAllister, W.T., Yokoyama, S., and Vassylyev, D.G. (2004). Cell *116*, this issue, 381–391.

Tyska, M.J., and Warshaw, D.M. (2002). The myosin power stroke. Cell Motil. Cytoskeleton *51*, 1–15.

Vale, R.D., and Milligan, R.A. (2000). The way things move: looking under the hood of molecular motor proteins. Science *288*, 88–95.

von Hippel, P.H. (1998). An integrated model of the transcription complex in elongation, termination, and editing. Science *281*, 660–665.

von Hippel, P.H., Bear, D.G., Morgan, W.D., and McSwiggen, J.A. (1984). Protein-nucleic acid interactions in transcription: a molecular analysis. Annu. Rev. Biochem. *53*, 389–446.

Wang, J., Sattar, A.K., Wang, C.C., Karam, J.D., Konigsberg, W.H., and Steitz, T.A. (1997). Crystal structure of a pol alpha family replication DNA polymerase from bacteriophage RB69. Cell *89*, 1087–1099.

Wang, D.M., Schnitzer, M.J., Yin, H., Landick, R., Gelles, J., and Block, S.M. (1998a). Force and velocity measured for single molecules of RNA polymerase. Science *282*, 902–907.

Wang, H.Y., Elston, T., Mogilner, A., and Oster, G. (1998b). Force generation in RNA polymerase. Biophys. J. *74*, 1186–1202.

Warnock, D.E., and Schmid, S.L. (1996). Dynamin GTPase, a force-generating molecular switch. Bioessays *18*, 885–893.

Wendt, T.G., Volkmann, N., Skiniotis, G., Goldie, K.N., Muller, J., Mandelkow, E., and Hoenger, A. (2002). Microscopic evidence for a minus-end-directed power stroke in the kinesin motor ncd. EMBO J. *21*, 5969–5978.

Yeagle, P.L., and Albert, A.D. (2003). A conformational trigger for activation of a G protein by a G protein-coupled receptor. Biochemistry *42*, 1365–1368.

Yin, Y.W., and Steitz, T.A. (2002). Structural basis for the transition from initiation to elongation transcription in T7 RNA polymerase. Science *298*, 1387–1395.

Yin, H., Wang, M.D., Svoboda, K., Landick, R., Block, S.M., and Gelles, J. (1995). Transcription against an applied force. Science *270*, 1653–1657.

Zhang, G., Campbell, E.A., Minakhin, L., Richter, C., Severinov, K., and Darst, S.A. (1999). Crystal structure of Thermus aquaticus core RNA polymerase at 3.3 A resolution. Cell *98*, 811–824.

Zhou, B.L., Pata, J.D., and Steitz, T.A. (2001). Crystal structure of a DinB lesion bypass DNA polymerase catalytic fragment reveals a classic polymerase catalytic domain. Mol. Cell *8*, 427–437.